Submitted to ApJ
Preprint typeset using LaTeX style emulateapj v. 5/2/11

ARCHITECTURE OF *Kepler's* MULTI-TRANSITING SYSTEMS: II. NEW INVESTIGATIONS WITH TWICE AS MANY CANDIDATES

Daniel C. Fabrycky[1,2], Jack J. Lissauer[6], Darin Ragozzine[7], Jason F. Rowe[5,6], Eric Agol[8], Thomas Barclay[6,10], Natalie Batalha[6,9], William Borucki[6], David R. Ciardi[11], Eric B. Ford[3], John C. Geary[7], Matthew J. Holman [7], Jon M. Jenkins [6], Jie Li[5,6], Robert C. Morehead[3], Avi Shporer[12,13], Jeffrey C. Smith[5,6], Jason H. Steffen[4], Martin Still[10]

Submitted to ApJ

ABSTRACT

Having discovered 885 planet candidates in 361 multiple-planet systems, *Kepler* has made transits a powerful method for studying the statistics of planetary systems. The orbits of only two pairs of planets in these candidate systems are apparently unstable. This indicates that a high percentage of the candidate systems are truly planets orbiting the same star, motivating physical investigations of the population. Pairs of planets in this sample are typically not in orbital resonances. However, pairs with orbital period ratios within a few percent of a first-order resonance (e.g. 2:1, 3:2) prefer orbital spacings just wide of the resonance and avoid spacings just narrow of the resonance. Finally, we investigate mutual inclinations based on transit duration ratios. We infer that the inner planets of pairs tend to have a smaller impact parameter than their outer companions, suggesting these planetary systems are typically coplanar to within a few degrees.

Subject headings: planetary systems; planets and satellites: detection, dynamical evolution and stability; methods: statistical

1. INTRODUCTION

Subsequent to the fortuitous discovery of an exoplanetary system around a pulsar via timing its pulses (Wolszczan & Frail 1992), the radial velocity technique has been the dominant contributor to our understanding of the architectures of planetary systems. This technique has revealed both systems with numerous planets and systems with dynamically rich architectures (Butler et al. 1999; Fischer et al. 2008; Rivera et al. 2010; Lovis et al. 2011) and enough planetary systems to perform statistical analyses of the ensemble (Wright et al. 2009). Given that multiple planets are the most frequent outcome of planet formation among the super-Earth and Neptune classes of planets (Mayor et al. 2011), the number of systems for study will continue to rise sharply as new Doppler sensitivities and time baselines are reached.

Nevertheless, the exoplanet community has just experienced a windfall of planetary systems via the transit technique, courtesy of NASA's *Kepler* mission. The *Kepler* team is in the process of vetting candidates to rule out false positives, with a special emphasis on multiplanet candidates, which has the promise of yielding a high-fidelity ($\gtrsim 98\%$) catalog of many hundreds of planetary systems (Lissauer et al. 2012).

Previously, the *Kepler* team presented planetary candidates discovered in the first four months of mission data Borucki et al. (2011a,b). Now, Batalha et al. (2012; hereafter B12) has identified candidates using the first 16 months of data. Contemporary with the previous catalog, Lissauer et al. (2011b) (hereafter Paper I) examined the dynamics and architectures of the candidate multiplanet systems. This paper extends the investigation of Paper I to the new catalog of candidates. It also pursues two additional studies: quantification of the fidelity of these systems based on their apparent orbital stability and the mutual inclinations of planets based on their transit duration ratios.

We begin by defining the sample of planet candidates (§ 2), in particular how we choose particular planet candidates to omit or update. Next (§ 3.1) we call attention to a few closely-packed planetary pairs and investigate two- and three-planet resonances. We discuss to what extent the sample of candidates obeys orbital stability constraints (§ 3.2), which has implications for its purity as being composed of real planetary systems (§ 3.3). The statistics of period ratios is examined in § 4. In § 5, we find that the transit duration ratios in multiplanet systems limit the typical mutual inclinations to just a few degrees. Finally, we recapitulate the results and draw comparisons to the Solar System (§ 6).

daniel.fabrycky@gmail.com
[1] Department of Astronomy and Astrophysics, University of California, Santa Cruz, Santa Cruz, CA 95064, USA
[2] Hubble Fellow
[3] Astronomy Department, University of Florida, 211 Bryant Space Sciences Center, Gainesville, FL 32111, USA
[4] Fermilab Center for Particle Astrophysics, P.O. Box 500, MS 127, Batavia, IL 60510, USA
[5] SETI Institute, Mountain View, CA, 94043, USA
[6] NASA Ames Research Center, Moffett Field, CA, 94035, USA
[7] Harvard-Smithsonian Center for Astrophysics, 60 Garden Street, Cambridge, MA 02138, USA
[8] Department of Astronomy, Box 351580, University of Washington, Seattle, WA 98195, USA
[9] Department of Physics and Astronomy, San Jose State University, San Jose, CA 95192, USA
[10] Bay Area Environmental Research Institute/NASA Ames Research Center, Moffett Field, CA 94035, USA
[11] NASA Exoplanet Science Institute / Caltech, 770 South Wilson Ave., MC 100-2, Pasadena, CA 91125, USA
[12] Las Cumbres Observatory Global Telescope Network, 6740 Cortona Drive, Suite 102, Santa Barbara, CA 93117, USA
[13] Department of Physics, Broida Hall, University of California, Santa Barbara, CA 93106, USA

2. THE SAMPLE

The sample is based on the KOI (*Kepler* object of interest) list in the appendix of B12. Stellar masses are obtained from the reported $\log g$ and stellar radius. We have not included some additional candidates given in the papers of Ford et al. (2012); Steffen et al. (2012); Fabrycky et al. (2012), as these were found by extraordinary searching beyond the standard pipeline applied to Q6 data.

In addition, we omitted a number of candidates for various reasons. Planets with uncertain transit periods from section 5.4 of B12 were omitted. We culled from the sample the same candidates mentioned in section 1 of Paper I. KOI-245.04 was discarded; it has low SNR (11.5) and poor reduced $\chi^2 = 2.11$, thus we attribute it to red noise.

We omitted planet candidates that are based on single transits, as their periods are too uncertain for the purposes of this paper; these are denoted by negative periods in B12.

For our analysis, we also revised the stellar and planetary properties of some candidates, as follows.

We updated the period of KOI-2174.03 as described in section 3.1.

In the new catalog, KOI-338 had a large change in stellar radius (1→19 $R_\odot$), due to $\log g$ determination using a new spectrum. There is no pulsational signal which generally accompanies a giant star, however, and the transit durations match much better with the radius of a dwarf star. We suggest either the spectroscopic result is in error, or the candidates are planets orbiting a background dwarf. For the stellar parameters we thus use a new analysis of the photometry in the *Kepler* Input Catalog (Brown et al. 2011), yielding $M_\star = 0.96 M_\odot$ and $R_\star = 1.65 R_\odot$. We scaled down the planet candidate sizes accordingly.

The stellar properties and radii of the planets in KOI-961 were updated to agree with Muirhead et al. (2012). Similarly, the depth of the transit signal is expected to closely match the fractional occulting area, and cases in which this is not true are likely poorly-conditioned fits. Planetary radii R_p are generally adopted from B12, but values outside the range 0.8-1.5 $R_\star\sqrt{\text{Depth}}$ were set to the nearest value of that range, using stellar radius $R_\star$ and Depth reported by B12. This caused a downward revision of 4 planet radii (KOI-377.01, KOI-601.02, KOI-1426.03, KOI-1845.02) and an upward revision of 1 planet radius (KOI-2324.01) for candidates within multiple systems.

With these changes from B12, the multiplicity statistics of systems of planet candidates are 1405 single systems, 242 double systems, 85 triple systems, 25 quadruple systems, 8 quintuple systems, and 1 sextuple system. The orbital period ratios (for section 4) and Hill spacings (for section 3.2) are given[14] in Tables 1-5. Overall, the number of multiple-planet systems approximately doubled from Paper I, and the biggest fractional increase was seen in the quadruples (8 → 25) and quintuples (1 → 8). We represent the periods and sizes of the systems of three or more planets in figure 1.

[14] Note that the labels "1", "2", etc. in these tables order the planets by increasing orbital period and do not always correspond to the planet discovery order of the KOI numbers ".01", ".02", etc.

3. DYNAMICS OF THE NEW SYSTEMS

Here we first discuss some special cases of planetary systems that are especially tightly packed, then step back to survey the stability properties and fidelity of the whole sample.

3.1. *Closely-spaced planets and other interesting systems*

Here we discuss some of the dynamically interesting systems that are present in the new dataset.

The closest new pair of new candidates are .01 and .04 in KOI-2248 with a period ratio of 1.065. In systems with transits detected at low signal-to-noise ratio, we must consider that some subset of the transits were not detected, or spurious transits were detected, modifying the period of the candidate (an alias). We checked aliases at periods 1/4, 1/3, 1/2, 2, 3, and 4 times the nominal period by polynomial-detrending with the transits masked out, then measuring the depth of the signal at locations implied by those periods. The signals are consistent with the reported periods for these planets. The pair (.01 and .02) would be hard-pressed to remain stable if both these planets are around the same star, the same situation as for KOI-284 (Paper I, Lissauer et al. 2012, Bryson et al. in prep; candidates 284.02 and 284.03 have a period ratio of 1.038). The likely alternatives are that (a) one or both candidates is actually a blended eclipsing binary, (b) the two are true planets, but orbiting different members of a wide binary star. One simple test we can consider is whether the ratio of orbital-velocity normalized transit durations:

$$\xi \equiv \frac{T_{\rm dur,1}/P_1^{1/3}}{T_{\rm dur,2}/P_2^{1/3}} \quad (1)$$

is near unity (where $T_{\rm dur}$ is the transit duration, P is the orbital period)[15], in which case it is more likely the planets are orbiting stars of equal density (perhaps the *same* star; Lissauer et al. 2012). For the unstable pairs in KOI-284 and KOI-2248, the value of ξ is 0.96 and 0.97 respectively, which does not provide independent evidence of them orbiting different stars. However, it suggests that if the planets are orbiting different stars in a physical binary, these two stars likely have similar type and might be resolvable – this has already been achieved for KOI-284 (Lissauer et al. 2012).

The next closest pair is KOI-2174, with a period ratio 1.1542 between .03 and .01. We performed the same alias check as above. Contrary to that case, every other transit of the smallest planet .03 is less deep and is marginally consistent with zero (509 ± 57 ppm versus 105 ± 63 ppm). Therefore we adopt the ephemeris BJD = $15.4502 \times E + 245509.8024$, where E is an integer, a period-doubling.

[15] Here and elsewhere, when referring to pairs of planets, we shall use "1" and "2" to denote the inner and outer planets of that pair respectively, even if there are other planets in the system and the specific pair is not the innermost two.

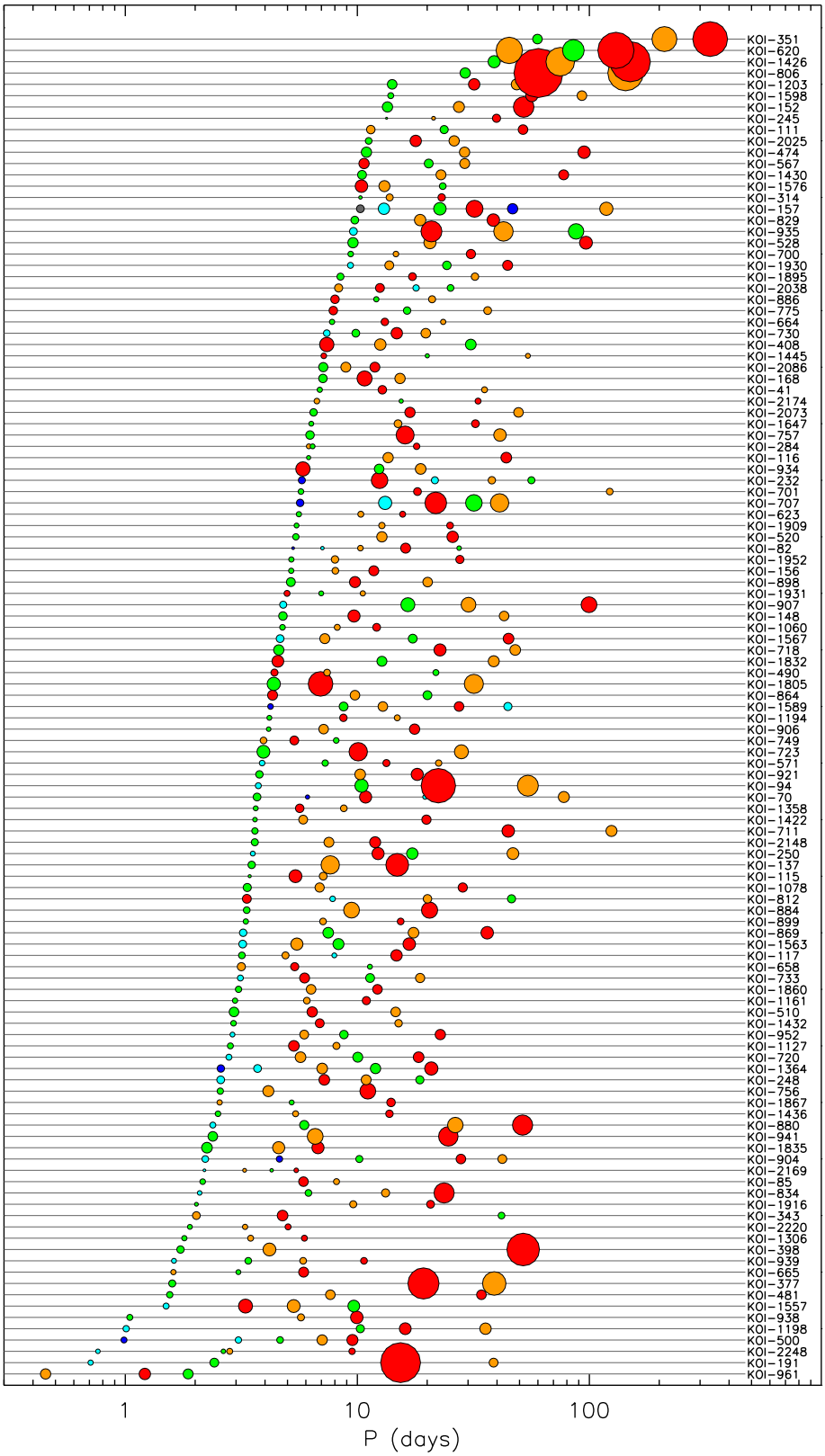

Figure 1. Systems of three or more planets. Each line corresponds to one system, as labelled on the right side. Ordering is by the innermost orbital period. Planet radii are to scale relative to one another, and are colored by decreasing size within each system: red, orange, green, light blue, dark blue, gray.

As we continue to wider period ratios, we no longer find reason to disbelieve the following systems are truly multiple planets orbiting an individual star, but note instead that their closely-packed nature makes them dynamically interesting.

KOI-1665 has a period ratio 1.17219 between .01 and .02. These are small candidates (1.2 and 1.0 $R_\oplus$) around a solar-type star, so the alias check above is not as powerful, however it raises no suspicion of the periods being incorrect. Given the planets' small sizes, they may also be small mass, so even this extreme period ratio may be dynamically stable on the long term.

KOI-262 has a nearly exact 6:5 commensurability, with a period ratio of 1.20010 ± 0.00003. The transits are well-defined, and we judge both candidates as secure detections at the correct periods.

All other planet pairs have period ratios > 1.25. In fact, in section 4, we will note that there may be a "pile-up" just wide of that period ratio, with sizes between Earth and Neptune. Kepler-11b and c (Lissauer et al. 2011a) is the confirmed example of this variety.

We also checked for potential 3-body resonances among planets in systems of higher multiplicity. Following Quillen (2011), we searched for small values of the frequency

$$f_{3-\mathrm{body}} = pf_1 - (p+q)f_2 + qf_3, \tag{2}$$

where f_1, f_2, and f_3 are the orbital frequencies (inverse periods) of three planets (estimated via the average transit periods) and p and q are integers. We recovered the resonant chain of KOI-730, four planet candidates with spacings near 4:3, 3:2, and 4:3 resonances as described by Paper I. We also found KOI-2086, whose three planets are also in a chain of first-order resonances, $f_1 : f_2 = 5 : 4$ and $f_2 : f_3 = 4 : 3$, an even more packed configuration. Here both pairs are offset by the same amount from the 2-body resonances:

$$4f_1 - 5f_2 = (-30 \pm 9) \times 10^{-5}\mathrm{day}^{-1}, \tag{3}$$

$$3f_2 - 4f_3 = (-26 \pm 5) \times 10^{-5}\mathrm{day}^{-1}, \tag{4}$$

such that the combined 3-body frequency $f_{3-\mathrm{body}}$, with $(p, q) = (1, 1)$, is $(1\pm1)\times10^{-5}\mathrm{day}^{-1}$. This is considerably closer to zero than its 2-body equivalents, suggesting it could have additional dynamical significance. Thus this case is intermediate between the chain of resonances in KOI-730 and the case of KOI-500 (as described in Paper I), whose planets are offset from the 2-body resonances, yet strongly in 3-body resonances. Another case of a three-body resonance is KOI-720. In that system there are no close 2-body resonances, yet the planets 720.01, 720.03, and 720.04 have $f_{3-\mathrm{body}} = -5f_{.01} + 3f_{.03} + 2f_{.04}$, of $(0 \pm 5) \times 10^{-5}\mathrm{day}^{-1}$. This is despite the period of .02 being intervening among them. Thus if this three-body resonance really has dynamical significance, it is despite the close presence of yet another planet.

There are two systems with candidate planets consisting of only one transit. KOI-490 is a 4-planet system including a possible gas giant displaying one transit. The single transit has a duration 4.9-6.8 times longer than the three short-period planets, suggesting that if $\xi \simeq 1$ (i.e. eccentricities are low and impact parameters are not near unity) the outer body's period should be ~ 1300 days. We do not include this additional planet in the remaining statistics of this paper, because its period is too crudely estimated; we analyze KOI-490 as a 3-planet system. The only other system with this trait is KOI-435, a 2-planet system. Since KOI-435.02 only displays one transit, we drop this system from the analysis altogether.

3.2. *Stability of Multiple-Candidate systems*

Next, we investigate stability of the candidate systems by proposing a mass-radius relationship, as in Paper I. It is subject to the caveats that (a) the planetary radii R_p scale with the uncertain stellar radii, and (b) we anticipate real planets have a diversity of structures (e.g., Wolfgang & Laughlin 2011). Nevertheless, we chose a simple power-law relationship for planetary masses $M_p = M_\oplus(R_p/R_\oplus)^\alpha$, where $M_\oplus/R_\oplus$ are the mass/radius of the Earth, $\alpha = 2.06$ for $R_p > R_\oplus$ and $\alpha = 3$ for $R_p \leq R_\oplus$. The choice for large planets is motivated by Solar System planets: it is a good fit to Earth, Uranus, Neptune, and Saturn. Continuing the power-law below Earth would mean smaller rocky planets are more dense, which is not likely a common outcome, so instead we choose a constant density (Earth's).

As noted in Paper I, in two-planet systems there exists an analytic stability criterion called Hill stability, in which the planets are forbidden from obtaining crossing orbits (e.g., Marchal & Bozis 1982). The relevant length scale is called the mutual Hill radius:

$$R_{H_{1,2}} = \Big[\frac{M_1 + M_2}{3M_\star}\Big]^{1/3} \frac{(a_1 + a_2)}{2}, \tag{5}$$

between two planets indexed by 1 and 2, M are their masses and a are their semi-major axes, and $M_\star$ is the mass of the stellar host. If the two planets begin on circular orbits with orbital separation in units of mutual Hill radius: $\Delta \equiv (a_2 - a_1)/R_{H_{1,2}} > 2\sqrt{3}$, then they are Hill stable (Gladman 1993). Values of Δ are given for the observed pairs in doubles in Table 1. All candidate systems obey this stability criterion, so we judge them to be plausibly stable.

There is no analytic stability criterion for the systems with more than two planets. However, in systems of three or more planets, instability time scales generally increase with separation, as in the two-planet case (Chambers et al. 1996). In Paper I, we numerically integrated all the previous catalog's systems of more than two planets, starting from circular, coplanar orbits with a power-law mass-radius relationship. In addition to each pair obeying two-planet stability criteria, we developed $\Delta_{\mathrm{in}} + \Delta_{\mathrm{out}} > 18$ as a conservative heuristic criterion, where the "in" and "out" subscripts pertain to the inner pair and the outer pair of three adjacent planets. In figure 2, we plot the Δs for inner and outer pairs of threesomes. There are a number of systems (Tables 2-5) with adjacent triples that do not satisfy that criterion (in addition to the pairwise criterion above). For all such systems that we have not already examined elsewhere (Paper I, Lissauer et al. 2012) — specifically, for KOI-620, 1557, and 2086 — we numerically integrated using *MERCURY* (Chambers 1999) as described in Paper I. We found them to be plausibly stable: starting on circular, coplanar orbits matching the phase and periods of the data, they suffered neither ejection, nor collision,

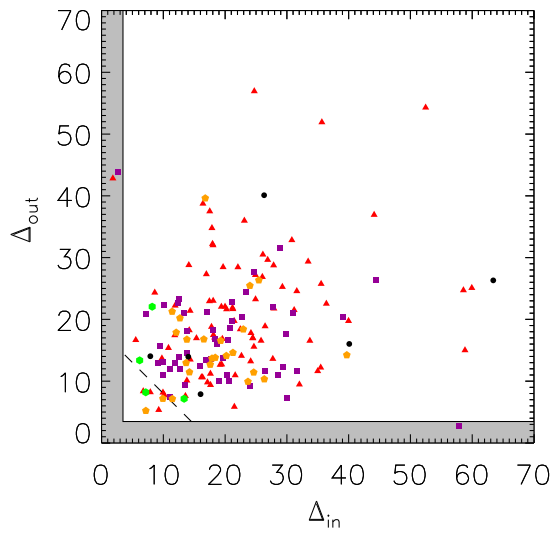

Figure 2. Separation of inner and outer pairs of triples (and adjacent 3-planet subsets of systems of multiplicity at or above 3), in units of the mutual Hill separation. The symbols denote planets in triples (red triangles), quadruples (purple squares), quintuples (orange pentagons), sextuples (green hexagons), and the Solar System (black dots). Systems with individual pairs that are unstable are the gray area: a triangle denoting KOI-284 and two squares denoting KOI-2248. Other systems show three planets with particularly close spacing (below the dashed line), but these were numerically integrated and found to be long-term stable.

nor a close encounter within 3 mutual Hill radii over a timespan of 10^{10} innermost orbits. We also integrated the new parameters (Muirhead et al. 2012) for KOI-961 for the same timespan and found them to remain stable.

The only new system that became unstable was KOI-2248, discussed above. Aside from the hybrid integrator, we also ran the Burlisch-Stoer integrator in *MERCURY* and the planets began violent gravitational scattering in several synodic time scales. Clearly, this system needs a qualitatively different understanding for its architecture, as described above.

One more system with at least one new planet appeared close to instability, KOI-707 = Kepler-33. Already in the discovery paper (Lissauer et al. 2012) an analysis of stability was carried out, so we performed no additional analysis here.

These outcomes of our stability analysis are for an adopted M_p–R_p relationship. To see how many systems would be unstable if the planets were denser, we considered various α values above and below $2R_\oplus$ (the approximate Super-Earth / mini-Neptune boundary) and recorded $\Delta < 2\sqrt{3}$ for any adjacent pairs. Below $2R_\oplus$, for any α below 6.9, no additional systems violate Hill's stability given circular orbits. Therefore all these planets may have a terrestrial structure, for which $\alpha \simeq 3.7$ (Valencia et al. 2006). For the region above $2R_\oplus$, no additional systems display instability for $\alpha \leq 2.6$ [i.e. $M_p = M_\oplus(R_p/R_\oplus)^{2.6}$], but at that value the pair of planets of KOI-523 and the outer two planets of KOI-620 would be unstable. Such a large α would imply an extreme density for gas-giant planets though, exceeding that of the core-heavy transiting planet HD 149026 (Sato et al. 2005). From this exercise, we see that our conclusions about stability are not sensitive to our adopted masses. We also see that stability considerations give us no additional insight into these planets' physical structure.

To summarize this stability study, for all the pairs of planet candidates, only two are expected to be unstable given low eccentricities and inclinations: KOI-284 and KOI-2248. Higher multiplicities do not appear unstable either, based on numerical integrations. If a mass-radius relationship favoring high density applies in reality, a few more systems could be unstable. We repeat the caveat that we have only considered instability while using initially circular orbits, and eccentric orbits could generally cause instability.

3.3. *Fidelity of Multiple-Candidate systems*

Morton & Johnson (2011) have emphasized that planet candidates from *Kepler*, once properly vetted, tend to be highly reliable ($> 90\%$), and Lissauer et al. (2012) extended and strengthened this statement for candidate multiple-planet systems. The density of background eclipsing binaries is so low, and the small depth and detailed shape of transits is so difficult to mimic given the photometric precision of *Kepler*, that a transit signal (particularly several transit signals) is quite unlikely to occur via a combination of stars only. Moreover, *Kepler's* exceptional signal-to-noise ratio and stability for centroid analyses means transit events occurring on background stars must lie very near the target star, in projection.

We can now address the statistical reliability of *Kepler's* multiplanet candidates from a new and independent angle: with so few candidate planetary systems showing instability (2 out of 885 pairs, including the higher-order multiples), we expect most of these candidates are truly in real systems. Consider the possibility that pairs are "false multis," defined as a system that appears to be a pair of planets around a star but is not. The most likely alternatives are (a) one or both members of the pair of candidates is a blended eclipsing binary, or (b) both members are planets, but they orbit different stars (Lissauer et al. 2012). In such "false multi" cases, there is no reason to expect the pair will obey stability constraints with respect to each other. Therefore we can calculate an expected rate of apparently unstable systems, given the hypothesis that all these candidate systems are false multis. If we draw two planets from the (P, $M_p/M_\star$) values of all the planet candidates in multis, and consider whether that pair would be stable if in the same system, $\Delta \leq 2\sqrt{3}$ occurs in $25182/391170 \simeq 6.4\%$ of the draws (the precise numbers come from exactly sampling all the possible pairs). That is, one would expect 57.0 to be unstable over the whole set of pairs. Using the Poisson distribution, to have found two or fewer unstable pairs given the expectation value $\lambda = 57.0$ has a probability of 3×10^{-22}. On the other hand, if only a fraction f of the systems are false multis, then the expected value of apparently unstable systems falls to λf. Given that only two systems in our sample appear to be unstable, we can place simple Bayesian constraints on the fraction f. Let us take a prior uniform in f from 0 to 1: $p(f) = 1$. Then we can apply Bayes' theorem to obtain the probability

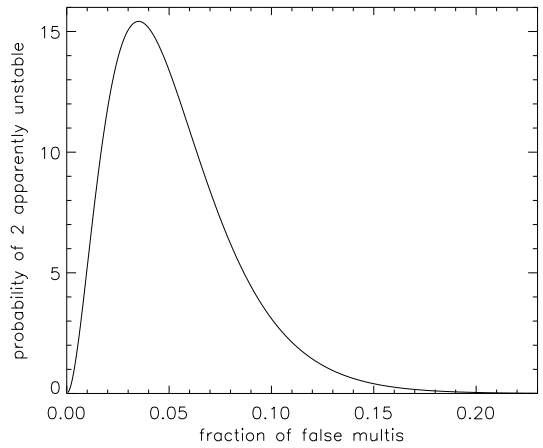

Figure 3. Probability distribution of the fraction of "false multis" given that we have found two pairs to be unstable.

of f given the observations:

$$P(f|\text{data}) = \frac{P(\text{data}|f)}{\int_0^1 df' P(\text{data}|f')}, \quad (6)$$

where $P(\text{data}|f)$ is the probability of the data given f, the only data we use is that we have found two apparently unstable systems, and f' is an integration variable which we marginalize over to determine the normalization. This probability distribution is given in figure 3, which shows a mode of 3.5% and a wide range of possible fractions: the 95% credible interval is 1.1% – 13%. This estimate is larger than the $\lesssim 2\%$ of the candidates in multiple systems not being true planets estimated by Lissauer et al. (2012). In the present estimate, we are counting planets that are around two different stars in a physically bound binary as a false multi, which as discussed above, may account for our unstable pairs KOI-284 and KOI-2248.

These estimates are based on drawing certain P and $M_p/M_\star$ values, which were in turn assumed to follow certain distributions, so let us examine those assumptions.

First, we have chosen a period distribution P matching the planet candidates in multiple systems. This distribution nearly matches the single-candidate period distribution, so this is appropriate if the false multi hypothesis is that a pair of planets are actually singles around hosts that are blended together. However, this distribution is narrower than the detached eclipsing binary distribution, which may be blended into some of the targets to produce the false multi signal. To explore this, we selected $M_p/M_\star$ as above (a reflection of the distribution of observed depths) but replaced the periods by two draws from the list of eclipsing binaries labeled "detached" by Slawson et al. (2011). This was done in a Monte Carlo fashion, resulting in an unstable fraction $\lambda/885 = 5.12\% \pm 0.04\%$. Given that this expectation is lower than above, the fraction of false multis would need to be higher to have produced two apparently unstable systems: the 95% credible interval is shifted to 1.5% – 16% under these different assumptions for the period ratio.

Second, we have adopted a particular mass-radius relationship, which gave $M_p/M_\star$. If the planets are actually denser than assumed, more would be deemed unstable, both from the observations and from the mock-systems simulations. These would likely scale in rough concert, and the conclusions regarding the fraction of false multiples rest on the ratio of those two. Therefore the main conclusion, that the strong majority of candidate planet pairs are likely true planets around the same star, would be robust to the mass-radius relationship chosen.

By considering stability, we have seen that $\approx 96\%$ of the pairs of multi-transiting candidates are actually planets around the same star. Recall that this is an independent estimate from Lissauer et al. (2012), who used binary statistics to estimate that in fully vetted systems, $\approx 98\%$ are real planets. In the following sections we therefore rely on this purity, assuming all the systems are real[16] while characterizing their architectures.

4. PERIOD RATIO STATISTICS

In figure 4 we plot the histogram of the period ratios ($\mathcal{P} \equiv P_2/P_1$) of all pairs in all systems, not just adjacent pairs. It spans a wide range, from quite hierarchical configurations, to the edge of stability. There is an apparent cut-off narrow of the 5:4 resonance, however KOI-262 is likely a true system at 6:5, suggesting this region is not totally empty. The main conclusion of Paper I is supported still: planet pairs are quite rarely in resonance. However, as resonances do have dynamical significance, we address their statistics presently.

To address the statistics of first-order resonances, we use the ζ_1 variable introduced in Paper I:

$$\zeta_1 = 3\left(\frac{1}{\mathcal{P}-1} - \text{Round}\left[\frac{1}{\mathcal{P}-1}\right]\right), \quad (7)$$

which describes how far away from a first-order resonance a pair of planets is. This variable has a value 0.0 at values of the period ratio $\mathcal{P} = (j+1) : j$, i.e. first-order resonances. Its value reaches -1 and $+1$ at the adjacent third-order resonances interior and exterior to the first-order resonance, i.e. at $(3j+2)$:$(3j-1)$ and $(3j+4)$:$(3j+1)$ respectively. The region between these third-order resonances is called the neighborhood of a particular first-order resonance. In figure 5 we plot the histogram of ζ_1, in which all values of j and all planetary pairs contribute. As in Paper I, we find that a value between -0.1 and -0.2 exhibits an excess: planetary pairs prefer to be just wide of first-order resonances with each other. We compare the observed $|\zeta_1|$ distribution to a random distribution, which is uniform in the logarithm of period ratios, via a K-S test. The null hypothesis is that period ratios are smoothly distributed, e.g. that they do not occur more often near ratios of integers (which correspond to dynamical resonances). A significant difference in these distributions is detected with p-value $= 6.5 \times 10^{-4}$: the systems do bunch towards the first-order resonance locations. In Paper I it was

[16] Because of their apparent instability, from this point on we cull KOI-284.02, KOI-284.03, KOI-2248.01, and KOI-2248.04. KOI-284 becomes a single-planet system and drops from the analysis, and KOI-2248 becomes a two-planet system and is analyzed as such.

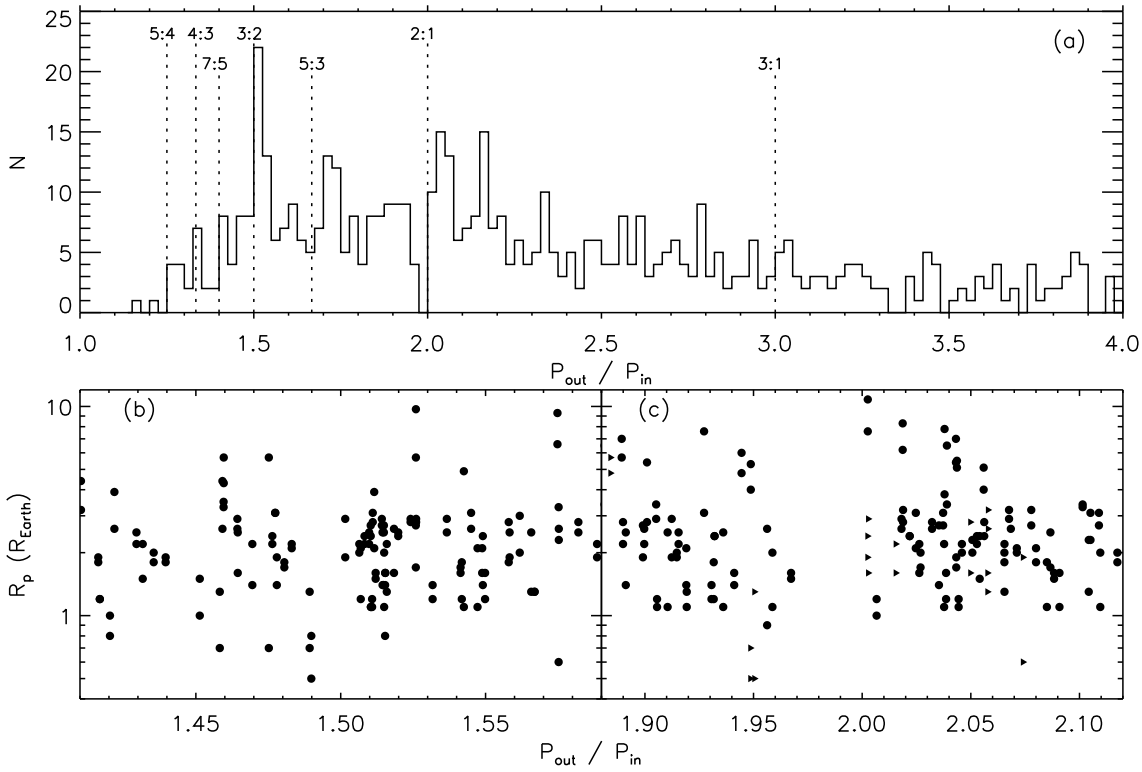

Figure 4. Period ratio statistics of all planet pairs. Panel (a): Histogram of all period ratios in the sample (i.e. pairwise between all planets in higher order multiples, not just adjacent planets), out to a period ratio of 4. First order (top row) and second order (lower row) resonances are marked. The mode of the full distribution is just wide of the 3:2 resonance, and there is an asymmetric feature near the 2:1 resonance. There is a sharp cut-off interior to the 5:4 resonance. Panel (b): Planetary radii versus the period ratio for planetary pairs near ($\Delta\mathcal{P} < 0.06\mathcal{P}$) the 3:2 resonance. Both radii for each pair are plotted. Panel (c): same as panel b, but near ($\Delta\mathcal{P} < 0.06\mathcal{P}$) the 2:1 resonance. Triangles denote planet pairs that are not adjacent, which have an intervening transiting planet.

found that a different variable, ζ_2, hinted that second-order resonances might similarly be bunched. However, we find with this expanded sample that $|\zeta_2|$ is consistent with a logarithmically-uniform distribution of period ratios, with K-S test p-value = 0.78. Nevertheless, there may certainly be individual systems (e.g., KOI-738 = Kepler-29, Fabrycky et al. 2012) which are in a dynamical second-order resonance. We describe a more general formalism for the ζ variable in appendix A, which gives context to our choice of equation 7 and will likely be useful in future investigations of the statistics of resonance.

Let us explore this preference for first-order resonances more. First, we compare the observed $|\zeta_1|$ distribution to a random distribution solely around the neighborhood of 2:1 (between 7:4 and 5:2) alone. The distributions significantly differ, with a p-value of 0.029, however this has weakened from 0.00099 (in Paper I) with the expanded sample including more small planets. The more important resonance contributing to the first-order resonance result is that systems in the neighborhood of 3:2 (between 10:7 and 8:5) tend to be near 3:2; $|\zeta_1|$ differs from a random distribution with a p-value of 0.0046. Looking back at panel a of figure 4, the global peak is just wide of the 3:2 resonance; a smaller peak exists just wide of 2:1. The peak at 3:2 appears to be a pile-up, in the sense that the spike is an excess on top of a baseline. The peak just wide of 2:1 contains only slightly more pairs than the trough just narrow of 2:1 is missing; this feature may imply an evolutionary "redistribution" determines this distribution more than a "pile-up" at the formation epoch. For a better view of these resonances, we plot scatter plots near these resonances in panels b and c of figure 4.

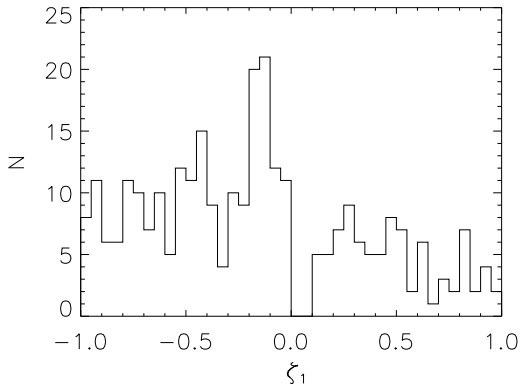

Figure 5. Histogram of ζ_1, a variable describing the offset from first-order resonances (eq. 7), for all planetary pairs in the neighborhood of a first-order resonance, i.e. with a period ratio between 1 and 2.5. The spike between -0.1 and -0.2 means that period ratios just wide of first-order resonances are overpopulated relative to random.

In panel b, we focus on the region near period ratios of 1.5, and in panel c, near 2.0. Just wide of 1.5, we note a striking pile-up (spanning 1.505 to 1.520 for $R_p \lesssim 3.0R_\oplus$). A similar over-density wide of 2.0 is apparent, but it is considerably more diffuse. These are the main features that make $|\zeta_1|$ non-random, as described above.

In these panels, we see more clearly the lack of pairs just narrow of the resonances, particularly for the 2:1 resonance. In both cases, this gap seems to be wider at larger planet sizes. Insofar as planet masses correlate with planet radii, this effect may be due to the fact that resonances are wider for more massive planets. To actually clear out these gaps, a dissipative effect needs to be invoked. This effect may simply be gravitational scattering, as in the case of the Kirkwood gaps in the asteroid belt: the resonance chaotically pumps up eccentricities (Wisdom 1983), and the bodies scatter off other planets, removing them from the resonance. Chaos was also noted by Murray (1986) in the 3:2 and 2:1 resonances at low eccentricity, which might be sufficient to produce the gaps in panels b and c. Another possibility is the action of tidal dissipation in the planet, pulling it towards the star and increasing the period ratio (Novak et al. 2003; Terquem & Papaloizou 2007). Yet another possibility is that, while the pair is still embedded in a gaseous disk, one planet may launch waves at its resonance location that interact with the other planet, preventing resonance capture (Podlewska-Gaca et al. 2012).

Last, we consider whether the pairs of planets close to first-order resonances are statistically closer to resonance than would be expected with random spacings. We have already discussed (pairwise going out in period): KOI-730 (4:3, 3:2, 4:3), KOI-2086 (5:4, 4:3), and KOI-262 (6:5); moreover KOI-1426.02/.03 are gas giants in 2:1 resonance. All these cases lie in the region $|\zeta_1| < 0.05$, however, they do not bunch to $\zeta_1 \simeq 0$ significantly more than random. So even though these pairs are so close to exact resonances ($\Delta\mathcal{P}/\mathcal{P} < 0.001$) and their dynamics is likely dominated by the resonance, they may be members of the smooth distribution of period ratios, and they do not necessarily point to differential migration which would produce a pile-up in resonance.

Our confidence is strengthened in systems with multiple, adjacent first-order resonances. We continue to take as the null hypothesis uniform spacing in $\log\mathcal{P}$, i.e. that near-resonant locations are not preferred. This spacing results in a nearly uniform distribution of ζ_1, which means that two adjacent period ratios have $|\zeta_{1,\rm in}|+|\zeta_{1,\rm out}|$ less than or equal to x with a probability $x^2/2$. (This is actually conservative estimate, as a logarithmic distribution of $\log\mathcal{P}$ yields slightly less probability than a uniform distribution at small ζ_1.) In the case of KOI-2086, the values of the two adjacent spacings are $\zeta_{1,\rm in} = -0.0324$ and $\zeta_{1,\rm out} = -0.0276$, so such systems would be this close to a first-order resonant chain only $p = 0.18\%$ of the time. However, given $n = 160$ sets of three adjacent planets, the expectation value that at least one of them will show such a close chain is $1-(1-p)^n = 25\%$, therefore KOI-2086's chain is rather expected even if planetary pairs do not prefer resonances. Having 4 planets in a resonant chain would be less expected, and having $|\zeta_{1,\rm in}|+|\zeta_{1,\rm mid}|+|\zeta_{1,\rm out}|$ (where subscript 'mid' refers to the middle pair) less than or equal to x occurs with probability $x^3/6$. For KOI-730, $\zeta_{1,\rm in} = -0.0123$, $\zeta_{1,\rm mid} = -0.0186$, $\zeta_{1,\rm out} = -0.0063$, and thus $p = 8.6\times10^{-6}$. There are $n = 43$ sets of 4 adjacent planets, so the expectation value that at least one would show such a chain is $1-(1-p)^n = 0.05\%$: a multi-resonant chain like that in KOI-730 is extremely unlikely if the orbital periods of planet candidates with a common host star were independent.

5. DURATION RATIO STATISTICS AND COPLANARITY

The durations in transiting planetary systems were recognized well before the *Kepler* launch to be a source for information on orbital eccentricity, as the eccentricity leads to changes in the orbital speed, and the duration is inversely proportional to projected orbital speed (Ford et al. 2008). Using the previous KOI catalog, Moorhead et al. (2011) performed such an analysis, finding evidence for moderate eccentricities among small planets. This result required knowledge of the stellar masses and radii. Several authors (Ragozzine & Holman 2010; Kipping et al. 2011) have also pointed out that in multiple planet systems, if one assumes that the planets are orbiting the same star, the properties of the star (most directly, its density) are probed by the durations and ingress and egress time scales of the transits. In such cases no detailed stellar model is needed, and constraints on the eccentricity of the planets is a by-product. Finally, it has been noted that gauging the relative transit durations of planets evident in the same lightcurve can serve as a means to validate them as planets around the same host star (Morehead et al. 2011; Lissauer et al. 2012, Morehead et al. in prep.). In these latter works, it is explicitly mentioned that a scaled duration should be equal between the planetary components to give high confidence that they are around the same star; we look into the details of that statement in this section.

Here we *assume* the planetary candidates are in true systems around the same star, and ask what the distribution of duration ratios tells us about coplanarity. In the limit that all the planetary orbits within a system are circular and coplanar, the normalized impact parameters b and semi-major axes a have the relationship:

$$b_2/b_1 = a_2/a_1 \quad [\textit{coplanar, circular}] \tag{8}$$

where 1 signifies an interior planet and 2 signifies an outer planet. Thus we expect that b_2 will be larger than b_1 in systems where both planets are quite coplanar and both transit. Conversely, we note that for the Kepler-11 g/e and Kepler-10 b/c and pairs, the observed b_2 is smaller than that given by equation 8, which means the orbits must be non-coplanar, to at least 1 degree and 5 degrees, respectively. Thus we expect the distribution of impact parameters can help us determine the distribution of mutual inclinations. For this method to have sensitivity, the typical mutual inclination must be $i \lesssim R_\star/a$, where $R_\star$ is the host's radius and a is a typical semi-major axis. We find below that, somewhat surprisingly, planetary systems are flat enough to fulfill this requirement.

We do not have accurate stellar properties or good knowledge of impact parameters themselves. However, transit durations $T_{\rm dur}$, from first to fourth contact, are well-measured and are $\simeq 2\sqrt{((1+r)^2-b^2)}R_*/v_{\rm orb}$, where $r = R_p/R_*$ and $v_{\rm orb} \propto P^{-1/3}$. Given the inner planet

will be biased towards smaller b if the planets are nearly coplanar, and in most cases $r \ll 1$, we expect the ratio of orbit-velocity normalized transit duration, ξ (eq. 1), to be *greater* than 1 for quite coplanar systems. Let us test the null hypothesis that planets around the same star are quite misaligned which would destroy such correlations, that their impact parameters are drawn from the same distribution. In such a case, $T_{\rm dur,1}/P_1^{1/3}$ and $T_{\rm dur,2}/P_2^{1/3}$ would follow the same distribution, therefore their ratios ξ or ξ^{-1} should also follow the same distribution as each other. We test that in figure 7, where the null hypothesis is that the black and red histograms agree. These histograms do not agree, with the center-of-mass of ξ lying at a significantly larger value than ξ^{-1}; a Kolmogorov-Smirnov (K-S) p-value of 5×10^{-15}. On the other hand, a model distribution consisting of perfectly coplanar and circular systems would lie entirely above 1, and measurement error introduces additional spread at the few-percent level only, so some mutual inclination or eccentricity is clearly needed.

There are potential biases which could affect this conclusion. First, the outer planet's r is typically larger (perhaps due to detection limits; Paper I), so this would bias ξ to values slightly less than 1, but we observe the opposite. Another aspect is that the box-least squares search that found most of these candidates (B12) was run over a range of durations $0.003P$ to $0.05P$. Planets outside this range were found sub-optimally; the search algorithm loses sensitivity to the very shortest durations (largest impact parameters) at long period and the very longest durations (smallest impact parameters) at short period. Therefore this effect biases ξ downwards, again against the observed trend. We have not identified any straightforward instrumental or analysis bias that pushes the distribution to larger ξ values, as observed.

To simulate the observed ξ distribution, we also should take into account photometric noise and eccentricities. With respect to photometric noise, the error on a duration measurement is $\sigma_{\rm dur} \simeq T_{\rm dur}\sqrt{2r}/SNR$ (Carter et al. 2008), typically $\sim 1\%$. We add a gaussian-random deviate with this standard deviation to the simulated durations. Eccentricity has two effects on the duration: (i) at a given inclination, it results in a different impact parameter and transit chord and (ii) the projected orbital speed changes; we model both these effects with Keplerian orbits. With these effects in place, the population model assumes mutual inclinations of planets are excited to a scale δ, and eccentricities of both planets are excited to a scale a factor n times δ. That is, the energy in the eccentricity epicycles is a certain number times equipartition with the energy in the inclination epicycles. Both the mutual inclination and eccentricity distributions are modeled as Rayleigh distributions, such that the Rayleigh widths are $\sigma_i = \delta$ and $\sigma_e = n\delta$. This allows us to construct a Monte Carlo method to determine predicted distributions of ξ as a function of δ and n. To evaluate this distribution, we make 250 mock systems for each observed pair of planets, where we have taken only the pairs where both planets are detected at SNR> 7.1, the nominal detection limit. For each mock system, step one is to draw the eccentricities: $e\sin\omega$ and $e\cos\omega$ are drawn from Gaussian distributions of width $n\delta$ (resulting in a uniform distribution of ω values and a Rayleigh distribution of e values). We discard a trial if either planets' eccentricity is above 1 or if the inner planet's apocenter distance exceeds the outer planet's pericenter distance, given their period ratio. Step two is to draw b_2 uniformly from $[0,b_{2,\rm max}]$, where $b_{2,\rm max}$ is the impact parameter the planet would need for the total SNR of the outer planet to drop to 7.1. This modeled SNR is taken as the observed SNR times the square root of the ratio between the modeled duration and the observed one. Step three is to draw b_1 from a distribution centered on $b_2(a_1/a_2)$ (eq. [8]) and having a gaussian width $\delta a/(R_\star + R_p)$. If $|b_1| > b_{1,\rm max}$, as above, this planet would not be detected in transit. If the conditions for acceptance are not met at each step, the process begins anew at step one. If accepted, the mock system's ξ value contributes to the simulated ξ distribution.

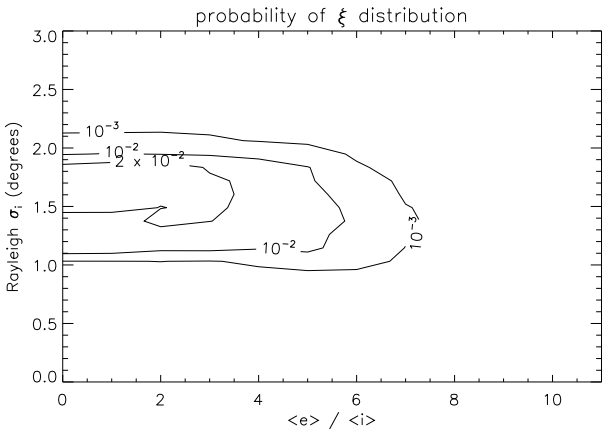

Figure 6. Kolmogorov-Smirnov p-value for inclined and eccentric systems. A region of acceptable probability lies in the range $\sim 1.0^\circ - 2.3^\circ$, for the Rayleigh parameter of the mutual inclination. The preferred value of eccentricity is near equipartition with the inclination, however the acceptable region (p-value=0.1%, equivalent to $3-\sigma$) spans a very wide range, from perfectly circular to 7 times equipartition.

Depending on the amount of inclination and eccentricity in the system, the simulated ξ distribution can be tuned to match the data. We computed a grid of models with steps of 0.002 in δ and 1 in n, and we show in figure 6 the p-value from the K-S test for these models. The peak (best-fit) value has a probability 0.027 and lies at $\delta = 0.032$, $n = 2$, corresponding to inclinations of $\sim 1.8^\circ$. The typical mutual inclinations lies firmly in the range $1.0^\circ - 2.3^\circ$: planetary systems tend to be quite flat.

In contrast to this narrow range of mutual inclination, the ξ distribution can be acceptably matched (p-value > 0.01) over a wide range of eccentricities. The geometrical reason for that is that if inclinations change by 1%, the duration may change by order unity, but if eccentricities change by 1%, the duration usually changes by only 1%. The result is that quite good fits can be obtained both for circular orbits and for eccentricities twice equipartition (the black models of figure 7, panels b and c respectively), and indeed up to many times equipartion. Therefore we do not claim to have detected eccentricity in these planet pairs, or provided any limits beyond that from transit durations of individual candidates (Moorhead et al. 2011), but we instead note that

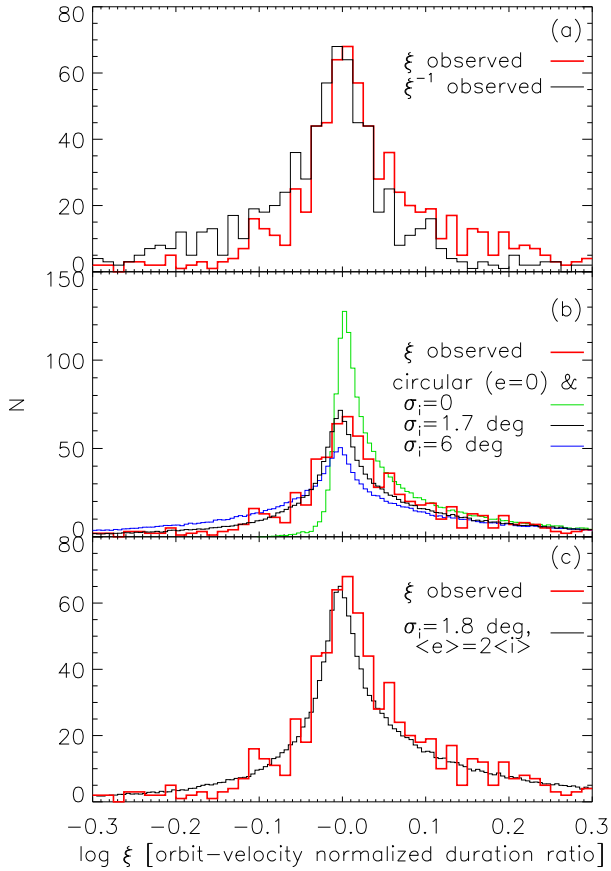

Figure 7. Histograms of normalized duration ratios (equation 1). Panel (a): the distributions of ξ itself and its inverse are contrasted. If planetary orbital planes are not correlated, these distributions would be equal. Instead, there is a signature of the inner planet having a longer duration, i.e. a smaller impact parameter. Panel (b): models of three different typical mutual inclinations, for circular orbits, are compared to the data, showing how these can be distinguished. Panel (c): the best-fitting model is compared to the data. This fit is not significantly better than the black line of panel b, as a wide range of eccentricities acceptably fits the data.

our conclusion about mutual inclination is not sensitive to these poorly known parameters.

Our conclusion that *Kepler's* planetary systems are flat was first investigated in Paper I, which used the number of planets of each multiplicity to show that the systems are likely quite flat (just a few degrees). However, it was possible that the typical inclination was higher than 10 degrees, in the case that planetary systems have many more planets ($\gtrsim 10$) than expected. To rule out the latter, the RV-sample was brought to bear to limit planet multiplicity (Tremaine & Dong 2011; Figueira et al. 2012), breaking the degeneracy and preferring small planetary inclinations of just a few degrees. This conclusion requires significant overlap between the current RV sample and the *Kepler* sample, which remains poorly quantified. Now, having reached the same conclusion from the *Kepler* sample alone, our confidence that planetary systems are typically flat is bolstered.

Nevertheless, some caveats apply to our investigation. We have used all pairs of planet candidates throughout, such that the n-planet systems are represented more, by a total of $n(n-1)/2$ pairs. Thus the architectures of larger-n systems carry more statistical weight. Nevertheless, by simulating all planet configurations and only comparing the doubly-transiting simulated pairs to the data, our determination of σ_i is unbiased. Another caveat is that the distribution of inclinations may not be well-characterized by a single Rayleigh distribution, and high-inclination components of the actual distribution would contribute less statistical weight. Thus, as with all applications of parameter-fitting, the limits given on the parameter σ_i hold only to the extent that a member of the family of model distributions describes the actual distribution.

6. DISCUSSION

Using the new catalog from *Kepler* doubling the numbers of planet candidates (B12), we have investigated the architecture of planetary systems anew. We have shown that the candidates avoid close orbital spacings that would destabilize real planets' orbits; from this we derived a likely fraction of $\approx 96\%$ of the candidate pairs are really pairs of planets orbiting the same star.

We found that planetary systems are usually not resonant but do show interesting clumping just wide of first-order resonances 2:1 and 3:2, and a gap just narrow of them. It is not yet clear whether formation mechanisms or evolution mechanisms account for this pattern.

The flatness of planetary systems, described based on multiplicity statistics by Paper I, was revisited here based on duration ratio statistics. We affirm and strengthen the result that pairs of planets tend to be quite well aligned, to within a few degrees. This new constraint uses the *Kepler* data alone, a more direct measurement than has been performed so far.

In future work (Ragozzine et al. in prep, Morehead et al. in prep), we will create population synthesis models, that propose an ansatz of planet distributions, run them through the selection functions of *Kepler*, and reproduce the planet multiplicities, period spacings, and duration ratios actually seen. This work serves as a stepping stone, as it has looked within the data itself for validation of the trends, by forming period and duration ratios.

6.1. *Comparison to the Solar System*

In this paper we have described the architecture of a set of multiple planets whose gross structure is completely alien. The sample is dominated by Neptunes and Super-Earths whose orbits are of order 10 days: nothing like that exists in the Solar System. In that sense, the *Kepler* sample of multiply-transiting planetary systems follows the trends of exoplanetary science over the past 20 years.

However, a striking feature of the Solar System is its extreme coplanarity. This property of planetary systems has only started being assessed (Paper I; Tremaine & Dong 2011; Figueira et al. 2012). Perhaps no observation is more crucial for theories of the Solar System's formation in a gaseous disk encircling the proto-Sun. For exoplanetary systems detected by radial velocity, there is typically no information on the inclination of individual planets, and only weak information (from stability, generally) available regarding their inclination with respect to one another. Thus it is exciting that, with the transit discoveries, we now have a statistical sample to assess the

degree of flatness of extrasolar systems. The remarkable conclusion is that the value for the spread in inclinations in the Solar System ($\sigma_i = 2.1^\circ - 3.1^\circ$, or $1.2^\circ - 1.8^\circ$ excluding Mercury, see appendix B) is very similar to the value from the exoplanets ($\sigma_i = 1.0^\circ - 2.3^\circ$). Moreover, although we have not demonstrated it with the data, we would expect the eccentricities of these planets to be roughly in equipartition with their mutual inclinations ($e \sim 0.03$), suggesting values compatible with the Solar System planets. Although the radial velocity technique has discovered many systems of super-Earths and Neptunes (Mayor et al. 2011), the population we are detecting here, their eccentricities have not yet been securely measured; we suggest they will turn out to be small. This is in contrast to the giant exoplanets found to date, but it may continue the trend that lower mass exoplanets have lower eccentricities (Wright et al. 2009).

Finally, we may ask whether the planets of the Solar System show any such resonant structure. The only pair close to a first-order mean-motion resonance is Uranus ($4.0 R_\oplus$) and Neptune ($3.9 R_\oplus$), whose period ratio is 1.96. These values lie near the border of the gap in panel c of figure 4. As the origin of this gap remains unclear, it is hard to know whether Uranus and Neptune's proximity to it has physical significance.

Funding for this mission is provided by NASA's Science Mission Directorate. We thank the entire *Kepler* team for the many years of work that is proving so successful. We thank Emily Fabrycky, Doug Lin, Man-Hoi Lee, and Scott Tremaine for helpful conversations and insightful comments. D. C. F. acknowledges support for this work was provided by NASA through Hubble Fellowship grant#HF-51272.01-A awarded by the Space Telescope Science Institute, which is operated by the Association of Universities for Research in Astronomy, Inc., for NASA, under contract NAS 5-26555. EA was supported by NSF Career grant 0645416. E.B.F acknowledges support by the National Aeronautics and Space Administration under grant NNX08AR04G issued through the Kepler Participating Scientist Program. This material is based upon work supported by the National Science Foundation under Grant No. 0707203. R.C.M. was support by the National Science Foundation Graduate Research Fellowship under Grant No. DGE-0802270.

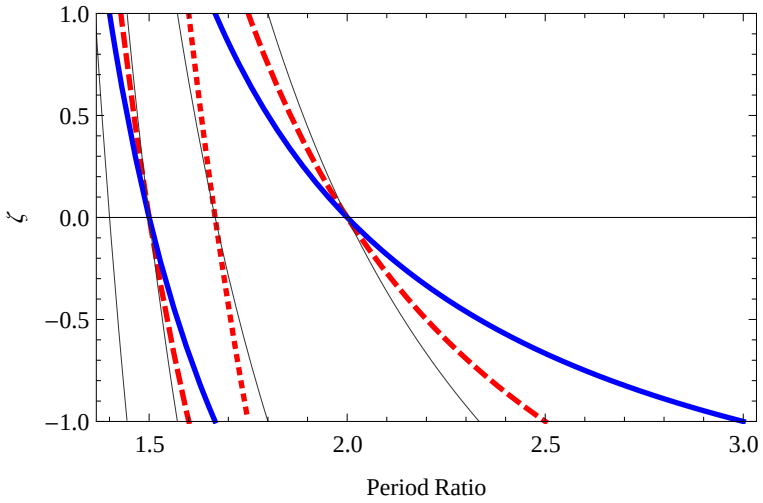

Figure 8. The value of ζ as a function of the period ratio of two planets. If only first order resonances are studied, then one uses $\zeta_{1,1}$ (solid, blue) where all period ratios are assigned to a neighborhood of a first-order resonance. If one simultaneously considers first and second-order resonances, then $\zeta_{2,1}$ (dashed, red) and $\zeta_{2,2}$ (dotted, red) are used where all period ratios are assigned either to the neighborhood of a first or a second order resonance (these are ζ_1 and ζ_2 of the main text). Finally, if one wishes to partition the real line into neighborhoods around only second order resonances, then $n = 1$ and $j = 2$ and the result is $\zeta_{1,2}$, the thin solid curves.

APPENDIX

REGARDING THE RESONANCE VARIABLE ζ

In this section we discuss in more detail the quantity ζ. The general form of ζ is given by

$$\zeta_{n,j} = (n+1)\left(\frac{j}{\mathcal{P}-1} - \text{Round}\left[\frac{j}{\mathcal{P}-1}\right]\right) \tag{A1}$$

where $\mathcal{P}$ is the ratio of the periods of the two planets (always greater than unity), j is the resonance order under consideration, and n is the number of resonance orders that are simultaneously being considered. This last statement means that the real line is partitioned into non-overlapping neighborhoods around MMRs up to order n. The boundaries between resonances are always defined by resonances of the lowest order not considered. The motivation for defining this quantity was to provide a means of treating equally all resonances under study, even though their neighborhoods are different sizes (approaching zero as the index $j \to \infty$).

For example, in Paper I and in section 4, both first and second order resonances are considered ($n = 2$) and the quantities ζ_1 and ζ_2 (here $\zeta_{2,1}$ and $\zeta_{2,2}$) are given by

$$\zeta_{2,1} = 3\left(\frac{1}{\mathcal{P}-1} - \text{Round}\left[\frac{1}{\mathcal{P}-1}\right]\right) \tag{A2}$$

and

$$\zeta_{2,2} = 3\left(\frac{2}{\mathcal{P}-1} - \text{Round}\left[\frac{2}{\mathcal{P}-1}\right]\right) \tag{A3}$$

where ζ_1 is applied to those planet pairs that fall into the neighborhoods of the first order resonances and ζ_2 is applied to the pairs in the neighborhoods of the second order resonances. The boundaries between these resonance neighborhoods is defined by the intermediate, third order resonances (the lowest order resonances not considered).

Suppose, however, that one wanted to assign all period ratios into the neighborhood of a first order resonance only, without considering second order resonances. Then the proper quantity is $\zeta_{1,1}$, which is contrasted to the $\zeta_{2,1}$ in figure 8. For our sample, choosing such a broad resonance neighborhood includes possible features in the continuum or near the second or higher order resonances and hence dilutes the power of the statistical tests we employ here. However, situations may arise where a selection criteria, such as examining only higher-index first order resonances such as 4:3, 5:4, etc., may justify the use of $\zeta_{1,1}$. Therefore we recommend it for future work with *Kepler*, as smaller planets are more likely to be found in such tightly packed configurations, and a longer baseline will have the sensitivity to see them. One other possibility would be to study only second order resonances (including 4:2 and 6:4), in which case one would use the $\zeta_{1,2}$ variable. Figure 8 contrasts these different choices for mapping period ratios into a space more suitable for studying resonances.

SOLAR SYSTEM MUTUAL INCLINATION DISTRIBUTION

Here we compute the best-fit Rayleigh distribution of the mutual inclinations for the Solar System planets. There are a total of $n(n-1)/2 = 28$ pairs for the $n = 8$ planets. We used on the Keplerian elements at J2000 provided by the JPL Solar System Dynamics website[17] to find the set of 28 mutual inclinations. This set was fit to a Rayleigh distribution, and the Rayleigh parameter constrained using the same Bayesian technique as section 3.3. The 95% credible interval was found to be $\sigma_i = 2.5^\circ|^{+0.6^\circ}_{-0.4^\circ}$. The planet Mercury is well-known as an outlier in inclination, and when this exercise is repeated just with the other 7 planets, the result is $\sigma_i = 1.4^\circ|^{+0.4^\circ}_{-0.2^\circ}$. These results were obtained with a uniform prior on σ_i, but since the allowed region is in each case rather narrow, the calculations are not sensitive to the prior. For a comparison of these results to the *Kepler* sample, see section 6.1.

Facilities: Kepler.

REFERENCES

Borucki, W. J., Koch, D. G., Basri, G., et al. 2011a, ApJ, 728, 117
—. 2011b, ApJ, 736, 19
Brown, T. M., Latham, D. W., Everett, M. E., & Esquerdo, G. A. 2011, AJ, 142, 112
Butler, R. P., Marcy, G. W., Fischer, D. A., et al. 1999, ApJ, 526, 916
Carter, J. A., Yee, J. C., Eastman, J., Gaudi, B. S., & Winn, J. N. 2008, ApJ, 689, 499
Chambers, J. E. 1999, MNRAS, 304, 793
Chambers, J. E., Wetherill, G. W., & Boss, A. P. 1996, Icarus, 119, 261
Fabrycky, D. C., Ford, E. B., Steffen, J. H., et al. 2012, ArXiv e-prints
Figueira, P., Marmier, M., Boué, G., et al. 2012, ArXiv e-prints
Fischer, D. A., Marcy, G. W., Butler, R. P., et al. 2008, ApJ, 675, 790
Ford, E. B., Quinn, S. N., & Veras, D. 2008, ApJ, 678, 1407
Ford, E. B., Fabrycky, D. C., Steffen, J. H., et al. 2012, preprint (arxiv:1201.5409)
Gladman, B. 1993, Icarus, 106, 247
Kipping, D. M., Dunn, W. R., Jasinski, J. M., & Manthri, V. P. 2011, ArXiv e-prints
Lissauer, J. J., Fabrycky, D. C., Ford, E. B., et al. 2011a, Nature, 470, 53
Lissauer, J. J., Ragozzine, D., Fabrycky, D. C., et al. 2011b, ApJS, 197, 8
Lissauer, J. J., Marcy, G. W., Rowe, J. F., et al. 2012, preprint (arxiv:1201.5424)
Lovis, C., Ségransan, D., Mayor, M., et al. 2011, A&A, 528, A112
Marchal, C., & Bozis, G. 1982, Celestial Mechanics, 26, 311
Mayor, M., Marmier, M., Lovis, C., et al. 2011, preprint (arxiv:1109.2497v1)
Moorhead, A. V., Ford, E. B., Morehead, R. C., et al. 2011, ApJS, 197, 1
Morehead, R. C., Ford, E. B., Prša, A., & Ragozzine, D. 2011, American Astronomical Society, ESS meeting #2, #28.01, 2, 2801
Morton, T. D., & Johnson, J. A. 2011, ApJ, 738, 170
Muirhead, P. S., Johnson, J. A., Apps, K., et al. 2012, ArXiv e-prints
Murray, C. D. 1986, Icarus, 65, 70
Novak, G. S., Lai, D., & Lin, D. N. C. 2003, in Astronomical Society of the Pacific Conference Series, Vol. 294, Scientific Frontiers in Research on Extrasolar Planets, ed. D. Deming & S. Seager, 177–180
Podlewska-Gaca, E., Papaloizou, J. C. B., & Szuszkiewicz, E. 2012, MNRAS, 2379
Quillen, A. C. 2011, MNRAS, 418, 1043
Ragozzine, D., & Holman, M. J. 2010, ArXiv e-prints
Rivera, E. J., Laughlin, G., Butler, R. P., et al. 2010, ApJ, 719, 890
Sato, B., Fischer, D. A., Henry, G. W., et al. 2005, ApJ, 633, 465
Slawson, R. W., Prša, A., Welsh, W. F., et al. 2011, AJ, 142, 160
Steffen, J. H., Fabrycky, D. C., Ford, E. B., et al. 2012, preprint (arxiv:1201.5412)
Terquem, C., & Papaloizou, J. C. B. 2007, ApJ, 654, 1110
Tremaine, S., & Dong, S. 2011, ArXiv e-prints
Valencia, D., O'Connell, R. J., & Sasselov, D. 2006, Icarus, 181, 545
Wisdom, J. 1983, Icarus, 56, 51
Wolfgang, A., & Laughlin, G. 2011, ArXiv e-prints
Wolszczan, A., & Frail, D. A. 1992, Nature, 355, 145
Wright, J. T., Upadhyay, S., Marcy, G. W., et al. 2009, ApJ, 693, 1084

[17] http://ssd.jpl.nasa.gov

Table 1
Characteristics of Systems with Two Transiting Planets (entire table is in the source)

KOI #	$R_{p,1}$ ($R_\oplus$)	$R_{p,2}$ ($R_\oplus$)	P_2/P_1	Δ
5	5.65	0.66	1.47518	8.2
46	4.32	0.96	1.72867	13.5
72	1.38	2.19	54.08308	87.9
89	4.87	6.47	2.45136	17.4
108	2.94	4.45	11.24943	44.5
112	1.20	2.86	13.77101	65.6
119	3.76	3.30	3.86939	26.9
123	2.64	2.71	3.27424	30.9
124	3.00	3.58	2.49937	21.2
139	1.49	7.33	67.26747	47.1
150	2.63	2.73	3.39808	28.7
153	2.07	2.47	1.87739	17.0
159	1.30	2.70	3.74052	39.1
171	2.67	2.07	2.19001	23.4
209	5.44	8.29	2.70221	13.9
216	1.49	7.15	2.68293	15.5
220	3.54	0.85	1.70309	14.0
222	2.03	1.66	2.02687	19.7
223	2.52	2.27	12.90608	54.3
238	2.40	1.35	1.54905	14.8
244	3.39	6.51	2.03899	12.6
251	2.65	0.84	1.38663	8.9
260	1.55	2.64	9.55471	61.3
262	2.20	2.79	1.20014	5.5
270	1.80	2.13	2.67619	30.9
271	2.48	2.60	1.65454	15.0
274	1.12	1.13	1.51041	21.1
275	1.95	2.04	5.20519	52.1
279	2.06	4.57	1.84618	13.4
282	1.18	3.36	3.25259	30.9
291	2.14	2.73	3.87681	36.5
304	1.11	4.89	1.54250	10.0
307	1.15	1.80	3.77548	51.9
312	1.91	1.84	1.41630	12.6
313	1.61	2.20	2.22082	25.5
316	2.72	2.94	9.95884	51.5
338	1.51	3.23	2.25601	21.9
339	1.55	1.66	6.48067	62.1
341	1.58	2.98	3.05158	30.5
369	1.14	1.08	1.71695	26.7
370	2.65	4.32	1.86849	14.7
379	2.58	1.83	3.44421	36.8
386	3.25	2.94	2.46264	21.0
392	1.33	2.27	2.64990	32.6
401	6.57	6.67	5.48026	22.0
413	2.75	2.10	1.62021	12.9
416	2.81	2.71	4.84703	35.4
427	4.31	2.65	1.74490	11.3
431	2.80	2.48	2.48550	22.0
433	5.60	12.90	81.43980	28.5
438	1.74	2.10	8.87876	52.7
440	2.36	2.26	3.19834	30.2
442	1.37	2.30	7.81624	60.8
446	1.76	1.72	1.70872	16.3
448	1.77	2.31	4.30085	34.8
456	1.50	3.27	3.17889	28.8
457	1.84	2.03	1.43543	11.1
459	1.24	3.09	2.81027	27.6
464	2.63	6.73	10.90841	33.4
471	1.04	2.29	2.73298	34.0
475	2.04	2.26	1.87181	17.3
497	1.53	2.74	2.98125	33.0
505	1.62	2.87	2.22206	22.0
508	3.44	3.31	2.10147	17.3
509	2.24	2.68	2.75106	26.7
511	1.26	2.25	1.87764	20.0
518	2.11	1.54	3.14698	32.2
519	2.43	2.53	2.85925	28.8
523	2.86	6.97	1.34073	5.0
534	1.67	2.43	2.33931	24.6
542	1.42	2.44	3.03135	32.9
543	1.39	2.23	1.37105	10.2
546	2.30	3.12	2.10507	20.1
551	1.98	2.23	2.04588	22.1
555	1.40	2.68	23.36546	69.6
564	2.62	6.09	6.07473	29.1
569	1.29	2.37	12.69431	65.3
572	1.24	2.44	2.15436	24.0
573	1.73	3.00	2.90831	28.9
574	1.14	2.45	1.93604	20.4
579	1.55	1.75	1.86286	21.7

Table 2
Characteristics of Systems with Three Transiting Planets

KOI #	$R_{p,1}$ ($R_\oplus$)	$R_{p,2}$ ($R_\oplus$)	P_2/P_1	$\Delta_{1,2}$	$R_{p,3}$ ($R_\oplus$)	P_3/P_2	$\Delta_{2,3}$
41	1.23	2.08	1.86083	23.1	1.40	2.75701	36.0
85	1.27	2.35	2.71933	35.0	1.41	1.38758	11.6
111	2.14	2.05	2.07117	21.2	2.36	2.18673	21.9
115	0.63	3.33	1.57522	13.6	1.88	1.31665	7.6
116	0.87	2.58	2.20129	26.1	2.68	3.23081	30.5
137	1.82	4.75	2.18034	16.4	6.00	1.94449	10.6
148	2.14	3.14	2.02469	17.9	2.35	4.43418	34.8
152	2.59	2.77	2.03215	19.2	5.36	1.90096	12.7
156	1.18	1.60	1.54982	16.2	2.53	1.46446	10.6
168	2.11	3.89	1.51156	9.9	2.62	1.42187	8.2
245	0.34	0.75	1.59358	36.4	2.00	1.86802	22.5
284	1.09	1.14	1.03830	1.8	1.49	2.80755	42.8
314	0.68	1.66	1.33641	10.8	1.77	1.67545	15.4
343	1.86	2.68	2.35246	24.7	1.58	8.78033	56.9
351	2.44	6.62	3.52522	21.5	9.32	1.57482	5.9
377	1.67	8.28	12.09936	32.0	6.16	2.01864	9.5
398	1.76	3.33	2.41710	22.1	8.66	12.40337	28.4
408	3.72	2.91	1.70156	11.9	2.70	2.45423	22.2
474	2.61	2.57	2.64821	26.9	3.24	3.27334	29.6
481	1.54	2.37	4.92295	44.1	2.44	4.47836	36.9
490	1.72	1.63	1.68583	17.5	1.40	2.94410	37.5
510	2.42	2.62	2.17289	20.2	2.38	2.28942	21.6
520	1.53	2.57	2.34861	24.5	2.93	2.01809	16.9
528	2.62	3.12	2.14612	18.0	3.27	4.70359	32.0
567	2.64	2.17	1.89968	17.1	2.53	1.42949	9.8
620	7.05	5.71	1.88931	9.3	9.68	1.52595	5.3
623	1.18	1.36	1.84837	25.8	1.42	1.51478	16.6
658	2.03	2.02	1.69812	17.0	1.14	2.10959	27.3
664	1.19	1.83	1.68814	20.0	1.19	1.78436	22.1
665	1.16	1.09	1.90558	31.2	2.51	1.91044	21.5
700	1.29	1.29	1.56691	18.1	2.28	2.10428	23.0
701	1.27	1.95	3.17836	35.7	1.57	6.73808	51.9
711	1.50	3.18	12.35005	58.6	2.83	2.78581	24.7
718	2.57	3.06	4.95356	40.0	2.67	2.10897	19.7
723	3.26	4.75	2.56257	17.8	3.61	2.78349	18.8
749	1.56	2.23	1.35740	9.8	1.33	1.51589	13.7
756	1.53	2.78	1.61086	14.3	4.06	2.68342	21.4
757	2.09	4.73	2.56977	18.3	3.21	2.56355	17.1
775	2.10	1.84	2.08001	19.4	1.86	2.22435	22.1
806	2.57	13.24	2.06841	7.9	9.52	2.37410	8.2
829	1.92	2.89	1.91233	18.1	3.17	2.06759	17.5
864	2.51	2.41	2.26525	21.5	2.23	2.05281	19.8
884	1.59	4.13	2.82940	22.6	4.23	2.16925	14.1
886	2.10	1.23	1.50690	11.8	1.74	1.73922	17.4
898	2.18	2.83	1.88991	15.4	2.36	2.05616	17.0
899	1.25	1.64	2.15140	24.9	1.61	2.16037	23.3
906	1.02	2.36	1.72542	17.5	2.60	2.46593	22.9
921	1.76	2.66	2.71716	27.7	3.09	1.76229	13.6
934	3.74	2.38	2.13023	17.6	2.73	1.51034	11.2
938	1.38	1.74	5.46504	58.8	3.16	1.74052	15.0
941	2.37	4.14	2.76224	21.3	5.10	3.74756	21.7
961	0.73	0.78	2.67770	33.7	0.57	1.53662	16.5
1060	1.34	1.36	1.72215	24.7	1.88	1.47794	15.6
1078	2.02	2.34	2.05070	18.0	2.33	4.13871	32.2
1127	1.38	2.66	1.87772	19.4	1.69	1.52592	12.7
1161	1.24	1.65	2.03860	26.5	2.00	1.80557	18.9
1194	1.08	1.82	2.08501	24.5	1.40	1.70686	17.0
1203	2.43	2.91	2.25665	21.6	2.79	1.52602	11.0
1306	1.25	1.39	1.93064	27.9	1.43	1.70531	21.8
1358	1.11	2.12	1.54722	14.4	1.56	1.54883	13.5
1422	1.03	2.18	1.61304	14.1	2.28	3.39804	28.8
1426	3.14	7.63	1.92722	10.1	10.81	2.00258	7.8
1430	2.17	2.50	2.18886	19.7	2.47	3.37915	28.5
1432	1.33	2.16	2.35246	29.3	1.75	2.18634	25.3
1436	1.34	1.44	2.16024	30.8	1.83	2.53756	32.8
1445	1.28	0.91	2.79257	52.5	1.12	2.71456	54.3
1576	3.20	2.84	1.25618	5.5	1.64	1.78386	16.7
1598	1.40	3.14	4.05393	35.5	2.39	1.64456	12.2
1647	1.06	1.92	2.36461	31.6	1.91	2.15601	24.6
1805	3.40	6.45	1.59105	8.6	4.97	4.57869	24.3
1832	2.95	2.55	2.80827	24.9	2.79	3.03365	27.2
1835	2.69	3.11	2.03724	17.6	3.08	1.47738	9.4
1860	1.52	2.44	2.05409	22.5	2.36	1.93204	18.4
1867	1.21	1.08	2.04438	27.9	2.15	2.68010	28.8
1895	1.74	1.92	2.04329	19.6	1.81	1.85954	16.8
1909	1.15	1.52	2.33221	35.5	1.63	1.96727	25.8
1916	0.82	1.69	4.74106	59.9	1.95	2.15406	25.1
1931	1.43	1.12	1.40392	14.2	1.24	1.51083	18.3
1952	1.23	1.83	1.54179	16.4	2.02	3.45365	38.7
2025	1.56	2.94	1.59510	13.8	2.61	1.46432	10.1
2073	1.80	2.60	2.60343	26.0	2.41	2.93633	26.9

Table 3
Characteristics of Systems with Four Transiting Planets

KOI #	$R_{p,1}$ ($R_\oplus$)	$R_{p,2}$ ($R_\oplus$)	P_2/P_1	$\Delta_{1,2}$	$R_{p,3}$ ($R_\oplus$)	P_3/P_2	$\Delta_{2,3}$	$R_{p,4}$ ($R_\oplus$)	P_4/P_3	$\Delta_{3,4}$
94	1.41	3.43	2.78467	28.5	9.25	2.14348	11.0	5.48	2.43118	12.0
117	1.58	1.70	1.54136	17.1	1.07	1.62358	21.1	2.93	1.85339	19.7
191	1.20	2.25	3.41293	39.1	10.67	6.35081	20.3	2.22	2.51658	11.1
248	1.85	2.72	2.79590	24.0	2.55	1.51489	9.2	1.99	1.70405	12.9
250	1.13	3.08	3.46601	30.0	2.94	1.40446	7.2	2.97	2.71449	20.9
571	1.31	1.53	1.86972	20.8	1.68	1.83606	18.6	1.53	1.67933	16.0
720	1.41	2.66	2.03533	19.7	2.53	1.76459	13.8	2.74	1.82941	14.5
730	1.56	1.89	1.33379	9.9	2.85	1.50156	11.1	2.43	1.33357	7.4
733	1.36	2.54	1.89120	18.4	2.21	1.91549	16.9	2.28	1.64273	13.5
812	2.19	1.29	2.34265	24.7	2.11	2.56366	27.7	2.02	2.30217	22.0
834	1.03	1.61	2.94412	44.5	1.98	2.14984	26.4	5.33	1.78742	11.6
869	1.75	2.73	2.32629	22.7	2.66	2.33114	20.4	3.20	2.07782	16.7
880	1.42	2.34	2.47684	28.8	4.00	4.48017	31.6	5.35	1.94873	11.7
907	1.66	3.64	3.44696	29.3	3.82	1.82467	12.3	4.08	3.30662	22.7
935	1.88	5.46	2.16923	16.0	5.07	2.04360	12.5	4.01	2.05591	13.8
939	1.13	1.57	2.09080	31.0	1.57	1.72345	21.0	1.65	1.82936	22.9
952	1.15	2.25	2.03771	20.7	2.15	1.48308	10.1	2.64	2.60289	22.3
1198	1.52	1.97	10.21309	75.1	2.97	1.56180	13.3	2.92	2.21750	21.1
1557	1.35	3.60	2.19839	19.0	3.27	1.61300	10.0	3.01	1.81594	13.2
1563	1.85	3.06	1.71184	13.6	2.80	1.51105	9.5	3.16	2.01881	15.7
1567	1.93	2.46	1.55829	12.6	2.22	2.39310	23.3	2.69	2.58806	24.4
1930	1.36	2.21	1.46948	13.8	2.14	1.77102	18.1	2.46	1.82766	18.3
2038	1.97	2.18	1.50640	12.7	1.54	1.43165	11.9	1.60	1.40778	12.9
2169	0.50	0.78	1.48984	29.8	0.74	1.30789	17.7	1.02	1.27635	13.6
2248	1.00	0.99	3.47299	57.9	1.39	1.06496	2.7	1.49	3.36783	43.8

Table 4
Characteristics of Systems with Five or Six Transiting Planets

KOI #	$R_{p,1}$ ($R_\oplus$)	$R_{p,2}$ ($R_\oplus$)	P_2/P_1	$\Delta_{1,2}$	$R_{p,3}$ ($R_\oplus$)	P_3/P_2	$\Delta_{2,3}$
70	1.92	0.91	1.64997	19.3	3.09	1.77980	16.6
82	0.52	0.70	1.33748	22.9	1.29	1.45825	18.4
232	1.73	4.31	2.16191	17.6	1.69	1.73170	12.7
500	1.38	1.53	3.11330	39.7	1.63	1.51206	14.2
707	1.83	3.42	2.32460	23.7	5.69	1.65274	9.9
904	1.65	1.46	2.08832	24.0	1.70	2.20868	25.5
1364	1.75	1.95	1.43956	12.1	2.69	1.89909	17.9
1589	1.27	2.23	2.06549	24.6	2.36	1.47638	11.4
157	1.89	2.92	1.26406	6.2	3.20	1.74179	13.4

Table 5
Characteristics of Systems with Five or Six Transiting Planets, Continued

KOI #	$R_{p,4}$ ($R_\oplus$)	P_4/P_3	$\Delta_{3,4}$	$R_{p,5}$ ($R_\oplus$)	P_5/P_4	$\Delta_{4,5}$	$R_{p,6}$ ($R_\oplus$)	P_6/P_5	$\Delta_{4,5}$
70	1.02	1.80373	16.8	2.78	3.96427	39.6			
82	2.45	1.56575	13.8	1.03	1.70038	16.8			
232	1.79	1.76016	20.2	1.69	1.48052	14.1			
500	2.64	1.51838	11.5	2.79	1.34997	7.1			
707	4.26	1.45961	7.2	4.77	1.29085	5.2			
904	2.43	2.74038	26.3	2.21	1.50821	10.3			
1364	2.59	1.69768	13.7	3.44	1.73927	13.0			
1589	2.41	2.12962	21.3	1.96	1.62371	14.6			
157	4.37	1.41032	7.1	2.60	1.45917	8.2	3.43	2.53526	22.1